

## Biased Transport of Elastic Cytoskeletal Filaments with Alternating Polarities by Molecular Motors

Barak Gur<sup>1</sup> and Oded Farago<sup>2</sup>

<sup>1</sup>*Department of Physics, Ben Gurion University, Be'er Sheva 84105, Israel*

<sup>2</sup>*Department of Biomedical Engineering, Ben Gurion University, Be'er Sheva 84105, Israel*

(Received 14 January 2010; published 7 June 2010)

We present a simple model for the bidirectional dynamics of actin bundles with alternating polarities in gliding assays with nonprocessive myosin motors. The bundle is represented as an elastic chain consisting of monomers with positive and negative polarities. The motion of the bundle is induced by the pulling forces of the underlying motors which stochastically attach to the monomers and, depending on their polarities, pull them in the right or left direction. We demonstrate that perfectly apolar chains consisting of equal numbers of monomers with positive and negative polarities may exhibit biased bidirectional motion with a nonzero drift. This effect is attributed to the elastic tension developed in the chain due to the action of the myosin motors. We also show that as a result of this tension, the attachment probability of the motors is greatly reduced and becomes strongly dependent on the length of the chain.

DOI: 10.1103/PhysRevLett.104.238101

PACS numbers: 87.16.Nn, 87.16.A-, 87.16.Ka, 87.16.Uv

Motor proteins are molecular machines that convert chemical energy into mechanical work by ATP hydrolysis. They “walk” on the microtubule and actin cytoskeleton and pull vesicles or organelles across the cell [1]. The intracellular transport of cargoes is achieved mainly by the action of individual motors which propagate along the cytoskeleton tracks in a direction determined by the intrinsic polarity of the filaments [2]. Other processes, such as cell motility and mitosis, require the cooperative work of many motors. Muscle contraction, for instance, involves the simultaneous action of hundreds of myosin II motors pulling on attached actin filaments and causing them to slide against each other [3]. One interesting outcome of cooperative action of molecular motors is their ability to generate bidirectional motion [4]. Bidirectional movement results from the competition between two populations of motors that work against each other in opposite directions [4–8]. The direction of motion flips from one direction to the other due to stochastic events of binding and unbinding of motors to the filament which tip the force balance between the two motor groups.

The dynamics of motor-filament systems are often studied using *in vitro* motility assays in which the filaments glide over a dense bed of immobilized motors and their motion is tracked by fluorescent microscopy [9]. Recently, we used such a motility assay to study the dynamics of actin bundles induced by the cooperative action of myosin II motors [10]. The bundles in these experiments were composed of short actin segments which, through a sequence of fusion events, assemble into filaments with randomly alternating polarities. Such apolar bundles exhibit “back and forth” bidirectional motion. We showed that the distribution of “reversal times” (i.e., the durations of unidirectional intervals of motion) take an exponential form  $P(\Delta t) \sim \exp(-\Delta t/\tau_{\text{rev}})$ , where  $\tau_{\text{rev}}$  is the character-

istic reversal time of the bidirectional motion [10,11]. Detailed analysis of the dynamics of many bundles revealed that  $\tau_{\text{rev}}$  is of the order of a few second and has no dependence on the length (number of monomers,  $N$ ) of the bundle. This result was in marked contradiction with previous theoretical models which predicted that  $\tau_{\text{rev}}$  grows exponentially with  $N$  [4]. To resolve this disagreement, we have introduced a model that takes into account the elastic energy stored in the actin bundle due to the action of the working motors [10,11]. The elastic energy modifies the rates at which motors attach to and detach from the actin and eliminates the exponential dependence of  $\tau_{\text{rev}}$  on  $N$ .

Our previous theoretical treatment of cooperative bidirectional motion was based on a mean field calculation of the actin elastic energy, ignoring both (i) the sequential order of the polarities of the monomers, and (ii) the positions along the filament where the pulling forces of motors are applied. The mean field elastic energy scales as  $E \sim NN_c$ , where  $N_c$  is the number of attached motors [10,11]. Within the mean field picture, the bidirectional motion on perfectly apolar tracks consisting of an equal number of monomers with right-pointing (“positive”) and left-pointing (“negative”) polarities has no bias; i.e., the intervals of motion in both directions occur with equal probability. In this Letter we discuss an interesting effect related to the elasticity of the actin. We show that apolar elastic filaments may exhibit a biased bidirectional motion and achieve a net migration along the motors-coated surface. For myosin II-actin systems, we find that the drift velocity is typically 2–3 orders of magnitude smaller than the velocity of a single myosin II motor and is comparable with the speed by which the motors move the apolar bundle cooperatively during the intervals of unidirectional motion. This newly identified mechanism of propagation may,

therefore, be relevant to processes of active self-organization of cytoskeletal structures during which filaments are transported and joined with each other by motor proteins.

To demonstrate the effect, we consider the chain illustrated in Fig. 1, consisting of  $N$  monomers connected by  $(N - 1)$  identical springs with a spring constant  $k$ . Each monomer may be either free and experience no pulling force ( $f = 0$ ), or attached to one motor in which case it is subjected to a force of magnitude  $f$  which is directed to the right ( $+f$ ) for monomers with positive polarities and left ( $-f$ ) for monomers with negative polarities. The moving velocity of the filament is given by  $V = f_{\text{total}}/\lambda$ , where  $f_{\text{total}} = \sum_{i=1}^N f_i$  is the sum of motor forces applied on the monomers and  $\lambda$  is the friction coefficient of the chain. A chain of  $N$  monomers has  $2^N$  connection configurations, where each such configuration can be represented by a vector  $\vec{C}$  of size  $N$  specifying the state (connected or disconnected) of each monomer. For example, a chain of 4 monomers in which the first and third monomers are connected to motors will be represented by  $\vec{C} = (1, 0, 1, 0)$ . Let us also introduce a vector  $\vec{S}$  whose components are related to the polarities of the monomers. The vector  $\vec{S} = (1, 1, -1, 1)$ , for instance, corresponds to a chain of 4 monomers in which the polarities of the first, second, and fourth monomers is positive while the third monomer has a negative polarity. The drift velocity can be calculated by averaging over all possible connection configurations of the motors (all possible values of the vector  $\vec{C}$ ):

$$V_{\text{drift}}(\vec{S}) \equiv \langle V \rangle = \sum_{j=1}^{2^N} \frac{f}{\lambda_j} (\vec{C}_j \cdot \vec{S}) P_j, \quad (1)$$

where  $P_j$  is the occurrence probability of the configuration, and the subscript  $j$  has been added to  $\lambda$  to account for possible variations in the friction coefficient between the different configurations. The probability  $P_j$  depends on (i) the number of attached motors in the configuration,

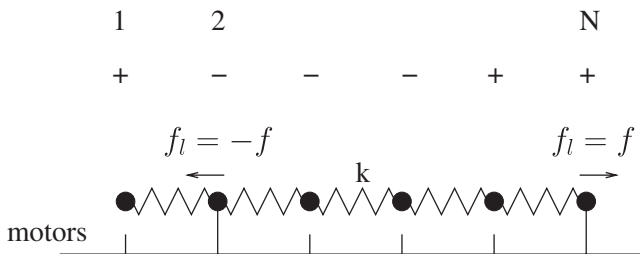


FIG. 1. A schematic drawing of the system: A chain of consisting of  $N$  monomers with alternating polarities, connected to each other by identical springs. The chain lies on a “bed” of motors, some of which are connected to the monomers. A connected monomer with positive (negative) polarity feels a pulling force of size  $+f$  ( $-f$ ). Disconnected monomers experience no force.

$N_c(j) = \|\vec{C}_j\|^2$ , (ii) the attachment probability of a single motor,  $q$ , and (iii) the total elastic energy of the springs  $E_j^{\text{el}}$ :

$$P_j = \frac{1}{Z} q^{N_c(j)} (1 - q)^{(N - N_c(j))} e^{-\beta E_j^{\text{el}}}, \quad (2)$$

where  $\beta = (k_B T)^{-1}$  is the inverse temperature and  $Z$  is the partition function of the system. The elastic energy is the sum of the energies of the springs,  $E_j^{\text{el}} = \sum_{i=1}^{N-1} F_i^2/2k$ , where  $F_i$  is the force stretching (or compressing) the  $i$ th spring. The forces  $F_i$  can be calculated using the following steps: (i) calculate the mean force  $\bar{f} \equiv f_{\text{total}}/N = f(\vec{C} \cdot \vec{S})/N$ , (ii) calculate the access forces acting on the monomers  $f_i^* = f C_i S_i - \bar{f}$ , and (iii) sum the access forces applied on all the monomers located on one side of the spring  $F_i = \sum_{l=1}^i f_l^* = -\sum_{l=i+1}^N f_l^*$ . Our analysis is based on the assumption that variations in  $\vec{C}$  (which occur when motors attach to or detach from the actin track) lead to instantaneous changes in the velocity of the filament which should always be proportional to the total exerted force. This assumption is expected to hold for low Reynolds numbers where inertia can be neglected.

Let us analyze the dynamics of a chain of size  $N = 4$ . There are six different apolar sequences for a chain of this length:  $\vec{S}_{1a} = -\vec{S}_{1b} = (1, 1, -1, -1)$ ,  $\vec{S}_{2a} = -\vec{S}_{2b} = (1, -1, 1, -1)$ ,  $\vec{S}_{3a} = -\vec{S}_{3b} = (1, -1, -1, 1)$ . It is easy to prove that the drift velocity [see Eqs. (1) and (2)] vanishes for the first four sequences which are antisymmetric with respect to reflection around the midpoint. This is not the case with the last two symmetric sequences. To see this, consider the sequence  $\vec{S}_{3a}$  and assume, for simplicity, that  $\lambda_j = \lambda$ . In the limit  $q \ll 1$ , one can ignore the configurations in which more than one out of the four monomers is connected to a motor. This leaves us with only five configurations: (i)  $\vec{C}_j = (0, 0, 0, 0)$ , for which  $V_j = 0$  and  $P_j = (1 - q)^4/Z$ , (ii)  $\vec{C}_j = (1, 0, 0, 0)$  and  $\vec{C}_j = (0, 0, 0, 1)$ , for which  $V_j = f/\lambda$  and  $P_j = q(1 - q)^3 e^{-(7/8)(\beta f^2/2k)}/Z$ , and (iii)  $\vec{C}_j = (0, 1, 0, 0)$  and  $\vec{C}_j = (0, 0, 1, 0)$ , for which  $V_j = -f/\lambda$  and  $P_j = q(1 - q)^3 e^{-(3/8)(\beta f^2/2k)}/Z$ . Substituting this in Eq. (2) gives  $V_{\text{drift}}(\vec{S}_{3a}) = -V_{\text{drift}}(\vec{S}_{3b}) \approx -2(f/\lambda)q[e^{-(3/8)(\beta f^2/2k)} - e^{-(7/8)(\beta f^2/2k)}]$ . For  $\beta f^2/2k \ll 1$  we find that the drift velocity increases with a third power of the motor force,  $V_{\text{drift}} \approx -(\beta/2k\lambda)f^3$ . This power law has a different exponent than 1—the scaling exponent for the velocity of stiff polar chains.

To further investigate this effect, we calculated the drift velocity for chains of  $N = 4M$  monomers with sequences

of the form  $\vec{S} = (\overbrace{-1, \dots, -1}^M, \overbrace{1, \dots, 1}^{2M}, \overbrace{-1, \dots, -1}^M)$ . Our results are summarized in Figs. 2(a) and 2(b). Figure 2(a) is based on a calculation in which the friction coefficient [see Eq. (1)],  $\lambda_j = \lambda_0 N$ , while in Fig. 2(b), we

assumed that  $\lambda_j = \lambda_0 N_c(j)$ . The results for  $N \leq 28$  have been derived using a full statistical calculation of the partition function, while for larger  $N$  they have been obtained from Monte Carlo simulations. The model parameters were assigned the following values which are representative of myosin II-actin systems [11,12]:  $\beta f^2/2k = 0.002$ ,  $q = 0.1$ , and  $f/\lambda_0 = 6 \mu\text{m}/\text{sec}$ . Both figures show that for small chains of size  $N < 200$ , the drift velocity increases rapidly with  $N$ . For larger chains ( $N > 200$ ),  $V_{\text{drift}}$  behaves differently in Figs. 2(a) and 2(b). In the former it decreases with  $N$ , while in the latter it saturates and increases again for  $N > 600$ . Note also that the different scales of the y axis in both figures. These differences can be attributed to the different values of  $\lambda_j$  used in the cases represented by Figs. 2(a) and 2(b). Since for each configuration, the ratio between the friction coefficients in both cases  $r_\lambda \equiv \lambda_j^B/\lambda_j^A = N_c(j)/N \leq 1$ , the drift velocity in (b) must always be larger than in (a). Figure 3 depicts the mean value of  $r_\lambda$  (i.e., the mean fraction of connected monomers) as a function of  $N$ . For  $N < 50$ ,  $\langle r_\lambda \rangle \simeq q = 0.1$  and, accordingly, the ratio between the drift velocities

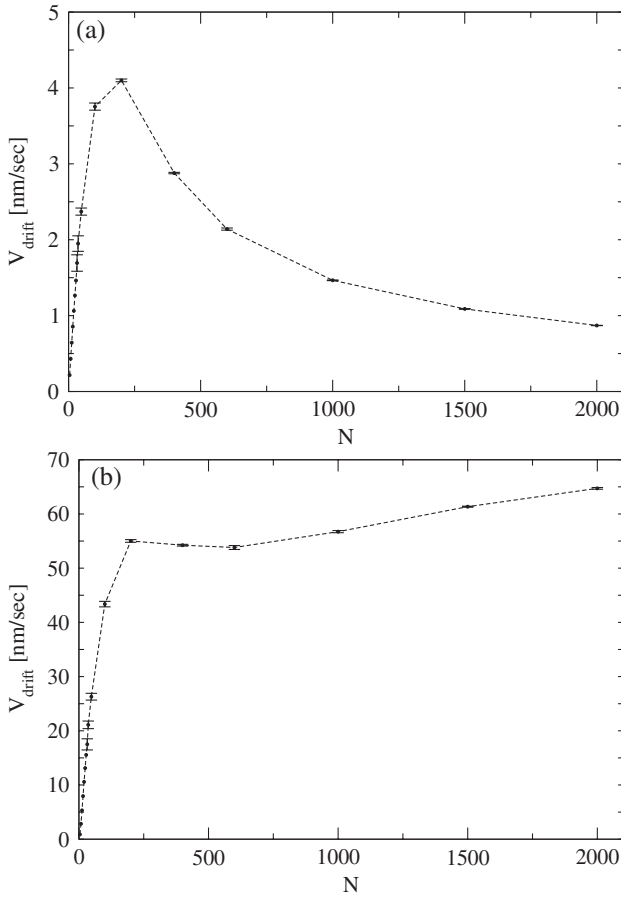


FIG. 2. The drift velocity  $V_{\text{drift}}$  as a function of the length of the chain. The friction coefficient  $\lambda_j$  is proportional to the number of monomers  $N$  in (a) and the number of connected motors  $N_c(j)$  in (b). The lines are guides to the eye.

in (b) and (a) in this regime is close to 1 order of magnitude. For  $N > 50$ ,  $\langle r_\lambda \rangle$  drops to values much smaller than  $q$ , which implies that the friction coefficient *per monomer* decreases with  $N$  in case (b) and explains why the drift velocity remains high and does not decrease sharply as in (a). The decrease in the mean fraction of connected monomers can be traced to the fact that configurations with larger  $N_c(j)$  have, in general, higher elastic energies and, therefore, smaller statistical weights. For the mean field elastic energy,  $E_j^{\text{el}}/k_B T = c(\beta f^2/2k)NN_c(j)$  [10,11], one gets

$$\langle r_\lambda \rangle = \left\langle \frac{N_c}{N} \right\rangle = \frac{q \exp(-cN\beta f^2/2k)}{1 - q[1 - \exp(-cN\beta f^2/2k)]}, \quad (3)$$

where  $c$  is a dimensionless constant of the order of 1. For  $c = 0.75$  and  $N \leq 1000$ , this expression (solid line in Fig. 3) gives a fair agreement with the computational results. For larger values of  $N$  (i.e., when  $\langle N_c/N \rangle$  becomes very small), the expression tends to overestimate the rate of decrease in the mean fraction of connected monomers (or, equivalently, the effective attachment probability). The decrease in the attachment probability of the motors is another, indirect, manifestation of cooperativity between the motors which is mediated through the forces that they jointly exert on the actin track. Equation (3) suggests that the elasticity of the track can be neglected for small filaments whose size  $N \ll (\beta f^2/2k)^{-1} \equiv N^*$ . In this regime, the two cooperativity effects discussed here which are associated with the elasticity of the actin filaments disappear: (i) The drift velocity  $V_{\text{drift}} \sim (\beta/2k\lambda)f^3 = (f/\lambda) \times (N^*/N) \ll (f/\lambda)$  is vanishingly smaller than the typical speed by which the bidirectionally moving bundle propagates in each direction, and (ii) the fraction of attached motors  $\langle N_c/N \rangle \simeq q$  is very close to the attachment probability of individual motors. The elasticity effects can be detected only for long filaments with  $N \gtrsim N^*$ , which are softer (the effective force constant of the filament decrease

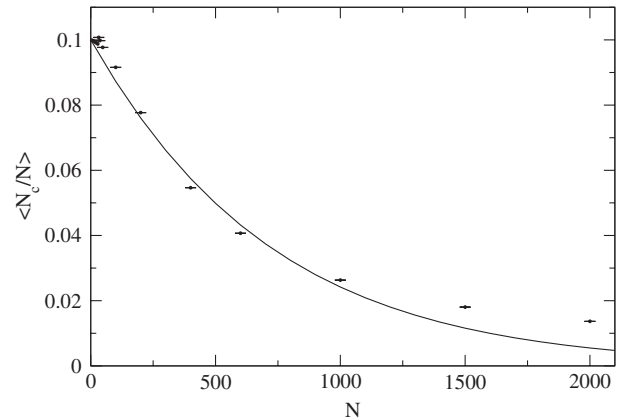


FIG. 3. The mean fraction of monomers connected motors,  $\langle N_c/N \rangle$  as a function of  $N$ . The solid line represents the mean field result Eq. (3) with  $c = 0.75$ .

as  $N^{-1}$ ) and, hence, more influenced by the forces of the motors. For infinitely stiff filaments ( $k \rightarrow \infty$ ), the cross-over filament size diverges ( $N^* \rightarrow \infty$ ) and the filament elasticity is, of course, irrelevant on all length scales.

Figures 2(a) and 2(b) represent two limiting cases. In the former, the friction is caused by the drag of the actin bundle in the viscous environment, while in the latter it originates from the attachment of the actin to the underlying surface of motors. The actual friction coefficient is expected to lie between these two extreme values and, therefore, the drift velocity should exhibit an intermediate behavior between those shown in Figs. 2(a) and 2(b). Thus, the typical magnitude of  $V_{\text{drift}}$  is expected to be of the order of 10 nm/sec. Interestingly, the drift velocity of the bundle is of the same order of magnitude as its speed during the bidirectional motion [10], which has also been found to be 2–3 orders of magnitude smaller than the moving velocity of individual myosin II motors ( $v \sim 6 \mu\text{m}/\text{sec}$  [12]). Over a period of a few minutes the apolar bundle may progress a distance of a few micrometers. This implies that the drift of apolar bundles may be relevant to the active remodeling of the cell cytoskeleton occurring during many cellular processes.

Our investigation of the role of the filament elasticity in modifying collective motion of molecular motors has been motivated by experiments which have been described and analyzed by using a ratchet model and a mean field approximation for the elastic energy [10,11]. In this paper we presented a more realistic microscopic based model that involves the determination of the exact elastic energy of the filaments. We demonstrated that such a model leads to new insights and novel results like the biased transport of filaments with no net polarities. Experimental verification of this surprising result is, however, difficult. It requires that (i) the moving filaments are perfectly apolar with internal (sequential) order, and (ii) that they move for sufficiently long period of time such that the net drift can be extracted from the statistics of the unidirectional intervals of motion. Unfortunately, the apolar bundles are not formed by a well controlled process, but rather through a sequence of stochastic fusion events that usually generate filaments with disordered, random, sequences and with little residual polarities [10]. Also, in the existing experimental setup, the bidirectional motion cannot be tracked for more than about 10 min, which is too short for a meaningful statistical analysis. What should be more experimentally testable is the other elasticity effect, namely, the reduction in the fraction of connected motors. This

effect, which has been attributed to the dependence of the elastic energy on the configuration of connected motors (denoted by the vector  $\vec{C}$ ), is not limited to apolar filaments. Polar filaments experiencing a nonuniform distribution of motor forces (i.e., when only a fraction of the monomers are connected to motors) will also develop a tensile stress that could potentially alter the attachment probability of the motors. In a future publication we plan to present a theoretical analysis of the attachment probability for perfectly polar filaments, similar to the analysis presented here for apolar filaments. We also plan to investigate this effect experimentally by using a motility assay combined with micro-manipulation technique (such as optical tweezers) to stall the gliding filament and measure the mean force generated by the motors. In the case of perfectly polar filaments, the forces of all the motors are applied along the same direction and, therefore, the total measured force should be simply proportional to the number of attached motors.

We thank Anne Bernheim-Groswasser for numerous valuable discussions. B. G. wishes to thank Amir Erez for his assistance with the numerical work and for many interesting discussions.

- 
- [1] B. Alberts, D. Bray, J. Lewis, M. Raff, K. Roberts, and J. D. Watson, *Molecular Biology of the Cell* (Garland, New York, 1994).
  - [2] *Guidebook to the Cytoskeletal and Motor Proteins*, edited by T. Kreis and R. Vale (Oxford University Press, New York, 1999).
  - [3] M. A. Geeves and K. C. Holmes, *Annu. Rev. Biochem.* **68**, 687 (1999).
  - [4] M. Badoual, F. Jülicher, and J. Prost, *Proc. Natl. Acad. Sci. U.S.A.* **99**, 6696 (2002).
  - [5] S. Klumpp and R. Lipowsky, *Proc. Natl. Acad. Sci. U.S.A.* **102**, 17 284 (2005).
  - [6] S. Muhuri and I. Pagonabarraga, *Europhys. Lett.* **84**, 58 009 (2008).
  - [7] D. Hexner and Y. Kafri, *Phys. Biol.* **6**, 036016 (2009).
  - [8] Y. Zhang, *Phys. Rev. E* **79**, 061918 (2009).
  - [9] J. R. Kuhn and T. D. Pollard, *Biophys. J.* **88**, 1387 (2005).
  - [10] B. Gilboa, D. Gillo, O. Farago, and A. Bernheim-Groswasser, *Soft Matter* **5**, 2223 (2009).
  - [11] D. Gillo, B. Gur, A. Bernheim-Groswasser, and O. Farago, *Phys. Rev. E* **80**, 021929 (2009).
  - [12] J. Howard, *Mechanics of Motor Proteins and the Cytoskeleton* (Sinauer Press, Sunderland, Mass, 2001).